



# 1 Long-term trends in agricultural droughts over Netherlands and 2 Germany: how extreme was the year 2018?

3 Yafei Huang<sup>1</sup>, Jonas Weis<sup>2</sup>, Harry Vereecken<sup>1</sup>, and Harrie-Jan Hendricks Franssen<sup>1</sup>

4 <sup>1</sup>Forschungszentrum Jülich, Agrosphere (IBG 3), Jülich, 52425, Germany

5 <sup>2</sup>The Hydrogeology Department, Karlsruhe Institute of Technology, 76131, Karlsruhe, Germany

6 *Correspondence to:* Yafei Huang (huangyafei136@yahoo.com)

7 **Abstract:** Droughts can have important impacts on environment and economy like in the year 2018 in parts of Europe.  
8 Droughts can be analyzed in terms of meteorological drought, agricultural drought, hydrological drought and social-  
9 economic drought. In this paper, we focus on meteorological and agricultural drought and analyzed drought trends for  
10 the period 1965-2019 and assessed how extreme the drought year 2018 was in Germany and the Netherlands. The  
11 analysis was made on the basis of the following drought indices: standardized precipitation index (SPI), standardized  
12 soil moisture index (SSI), potential precipitation deficit (PPD) and ET deficit. SPI and SSI were computed at two time  
13 scales, the period April-September and a 12-months period. In order to analyze drought trends and the ranking of the  
14 year 2018, HYDRUS 1-D simulations were carried out for 31 sites with long-term meteorological observations and  
15 soil moisture, potential evapotranspiration (ET) and actual ET were determined for five soil types (clay, silt, loam,  
16 sandy loam and loamy sand). The results show that the year 2018 was severely dry, which was especially related to  
17 the highest potential ET in the time series 1965-2019, for most of the sites. For around half of the 31 sites the year  
18 2018 had the lowest SSI, and largest PPD and ET-deficit in the 1965-2019 time series, followed by 1976 and 2003.  
19 The trend analysis reveals that meteorological drought (SPI) hardly shows significant trends over 1965-2019 over the  
20 studied domain, but agricultural droughts (SSI) are increasing, at several sites significantly, and at even more sites  
21 PPD and ET deficit show significant trends. The increasing droughts over Germany and Netherlands are mainly driven  
22 by increasing potential ET and increasing vegetation water demand.

23

## 24 1 Introduction

25 Drought is a climatic phenomenon that is expected to increase in frequency and severity over Europe in  
26 the future and is related to the ongoing climate change (Seneviratne et al., 2012a; Orłowsky and  
27 Seneviratne, 2013; Mukherjee et al., 2018; Samaniego et al., 2018; Pokhrel et al., 2021). Droughts are  
28 considered to be the most damaging natural hazard after floods, when measured globally in terms of the  
29 population affected, suffering more than 2.2 million victims from 1950 to 2014 (Mishra and Singh, 2010;  
30 Guha-Sapir, 2015; Zink et al., 2016). Droughts have a negative impact on food production, and shortage of  
31 water supply, making it the costliest disaster in Europe in general (AghaKouchak, 2014; Guha-Sapir et al.,  
32 2015; Zink et al., 2016).

33 We distinguish between meteorological, hydrological, agricultural and socio-economic drought, in  
34 correspondence with Mishra and Singh (2010), Wilhite and Glantz (1985) and AMS (2004). Meteorological  
35 drought is related to a period with rain deficiency with respect to the long-term average precipitation, and  
36 is usually assessed by a standardized precipitation index (SPI) (AMS, 2004). Hydrological drought is  
37 characterized by a river discharge deficit or low groundwater level (Wilhite and Glantz, 1985). Agricultural  
38 drought is defined in terms of soil moisture deficit, leading to crop yield reductions (Anderson et al., 2016).  
39 Agricultural drought and hydrological drought are affected by meteorological drought but not necessarily,  
40 and with a certain delay with a typical time lag of a month or a few months. Hydrological drought and



41 agricultural drought usually lead to shortage of water supply for residents and jeopardize food security  
42 and cause economic damages. Therefore, socio-economic drought is related to the mentioned three  
43 drought indices.

44 Historical drought events like for the years 1976, 1996, 2003 and 2015 in Europe have been widely  
45 investigated in literature, and it was concluded that these droughts had severe consequences for  
46 agriculture, riverine transportation and drinking water (Sheffield and Wood, 2007; Mühr et al., 2018; Bakke  
47 et al., 2020; Buitink et al., 2020; Buras et al., 2020). In Germany, huge economic losses have been reported  
48 related to the record breaking temperatures and severe drought in the summer 2018 and this affected  
49 agriculture, tourism and shipping losses (Mühr et al., 2018).

50 Analysis of droughts and studies on drought trends since the 1950s have been conducted (Sheffield and  
51 Wood, 2007; Sheffield et al., 2012; Bakke et al., 2020). Barker studied droughts based on standardized  
52 stream flow index for the period 1891 to 2015 for the UK and identified extreme droughts like the 1976  
53 drought and also periods with multiple and longer droughts (e.g. early 1940s and early 1970s) at the  
54 catchment scale (Barker et al., 2019). No consistent global drought trends were found and the trends  
55 generally differ from region to region (Sheffield and Wood, 2007; Orłowsky and Seneviratne, 2013; Spinoni  
56 et al., 2015). Sheffield and Wood (2007) showed that droughts increase in frequency and magnitude  
57 globally but trends differ, depending on the drought index used. Orłowsky and Seneviratne (2013)  
58 investigated the standardized precipitation index (SPI) as an indicator for meteorological drought for  
59 observation datasets and simulations from the 5th phase of the Coupled Model Intercomparison Project  
60 (CMIP5) and the results showed that frequency of droughts has increased in the Mediterranean, South  
61 Africa and Central America/Mexico over the past decades and this trend would continue in the 21<sup>st</sup> century  
62 according to CMIP projections (Orłowsky and Seneviratne, 2013). In Europe, the SPI-based analysis  
63 indicates that droughts in northern Europe have been mitigated while in southern Europe the magnitude  
64 of droughts have increased (Gudmundsson and Seneviratne, 2015). However, no consistent trends over  
65 central Europe were found (Gudmundsson and Seneviratne, 2015; Spinoni et al., 2015).

66 In addition to drought trends, individual historic drought events also have been widely studied (Ciais et al.,  
67 2005; Seneviratne et al., 2012b; Zink et al., 2016; Laaha et al., 2017; Bakke et al., 2020; Buitink et al., 2020;  
68 Buras et al., 2020). For Central Europe the years 1976 and 2003 were affected by the most severe droughts  
69 over the last 50 years (Ciais et al., 2005; Teuling et al., 2013). These two years gathered much attention  
70 from media and were generally used as reference for recent drought events. The year 1976 suffered soil  
71 moisture deficit and in central Europe the 2003 summer drought was more severe than the year 1976  
72 (Teuling et al., 2013). The year 2003 witnessed a 30% reduction in primary productivity which was a  
73 consequence of precipitation deficit and extreme heat waves (Ciais et al., 2005). Drought events in 1996  
74 and 2015 were also analyzed in studies (Laaha et al., 2017; Barker et al., 2019). Barker showed that the  
75 drought event 1995-1996 was the worst drought in central northern England since 1891 (Barker et al.,  
76 2019). In 2015, drought also affected large parts of Europe and especially the Eastern part of Europe  
77 (Laaha et al., 2017). The year 2018 also drew much attention from media and scientists and is considered  
78 to be one of the most extreme drought years and is analyzed and discussed in this paper. From climatic-  
79 data-based SPI it was found that northern Europe experienced an extreme drought in 2018 (Bakke et al.,  
80 2020; Graf et al., 2020). Buitink et al. (2020) found, with help of an analysis based on in-situ data and  
81 remote sensing data, that Netherlands witnessed in 2018 low soil moisture contents related to low  
82 precipitation, which reduced ET (Buitink et al., 2020). However, until now it was not explored completely  
83 how exceptional the year 2018 was in Germany and the Netherlands in terms of different drought indices.  
84 This paper not only analyzes meteorological drought, but also agricultural drought with help of four



85 drought indices for Germany and the Netherlands. The drought analysis was based on HYDRUS 1-D  
86 simulations using long-term observed climatic data as model forcing and using five different soil types  
87 which are clay, silt, loam, loamy sand and sandy loam out of 12 textural soil classes. These five soil types  
88 cover well the soil texture triangle and therefore the different types of soils. This modeling provides a  
89 better understanding of drought trends and the 2018 drought event for 31 different locations over the  
90 Netherlands and Germany with long-term meteorological observations. In situ measured soil moisture  
91 data and remotely sensed soil moisture are not available for such long time series and are in general  
92 strongly affected by measurement uncertainties. Atmospheric reanalysis also provides soil moisture data,  
93 but soil moisture is not an objective of such a reanalysis, and it is modelled at a relatively coarse scale and  
94 with a simplified process representation. Therefore, simulated soil moisture content by a soil hydrological  
95 model, driven by observed meteorological data, is expected to give the most reliable information on long  
96 term (agricultural) drought trends. In this work, we analyzed calculated potential and actual  
97 evapotranspiration (ET) as well as root zone soil moisture in detail. These three variables together with  
98 precipitation were used to determine four drought indices: SPI, standardized soil moisture index (SSI),  
99 potential precipitation deficit (PPD) and ET deficit. With the time series of the above-mentioned variables,  
100 drought trends were analyzed, including the mechanisms behind the observed trends. In addition, it was  
101 analyzed how extreme the 2018 drought event was in a historical context. The drought statistics and trends  
102 were analyzed for different soil types, in order to determine whether drought trends were different for  
103 the different soil types.

104 In Sect.2, we introduce the climatic stations over Germany and the Netherlands for which drought  
105 assessments were made in this study, and also the model HYDRUS to simulate water flow in soils and  
106 evapotranspiration is introduced. In addition, the study design and the four drought indices are introduced.  
107 In Sect.3, we present the results of the drought trend analysis with a focus on extreme events and the year  
108 2018. In Sect.4, we discuss and compare the drought trends and the extreme events with results from  
109 other studies. Also limitations of this study are discussed. In Sect.5, we summarize this work with the most  
110 important conclusions.

111

## 112 **2 Data and Methodology**

### 113 **2.1 Climatic data preparation**

114 In this study, 26 meteorological stations in Germany and 5 in the Netherlands were selected to investigate  
115 drought trends over the period 1965-2019 and the uniqueness of the 2018 drought event in this region.  
116 The stations are grouped in order to analyze domains with more similar climatological conditions:  
117 Netherlands, northern Germany, western Germany, eastern Germany and southern Germany as shown in  
118 the table 1.

119

120 **Table 1.** Analyzed meteorological stations and assignment to different domains.

Domains	Sites
North Germany	Bremen, Bremerhaven, Hamburg, Hannover, Helgoland, List auf Sylt and Soltau



West Germany	Aachen, Essen, Gießen-Wettenberg, Köln-Bonn, Saarbrücken and Trier
East Germany	Artern, Chemnitz, Lindenberg, Potsdam, Magdeburg, Rostock-Warnemünde and Schwerin
South Germany	Augsburg, Freiburg, Hof, Nürnberg, Öhringen and Regensburg
Netherlands	Eelde, De Kooy, De Bilt, Vlissingen and Maastricht

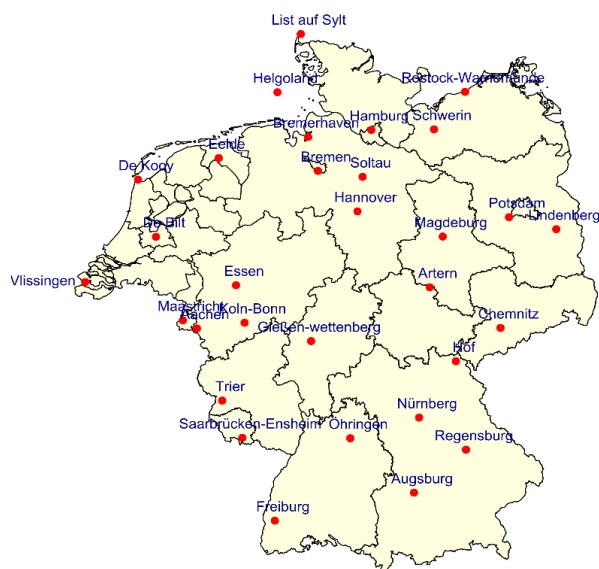
---

121

122 Figure 1 illustrates the spatial distribution of the meteorological stations. The meteorological stations are  
123 located between 0 m above sea level (De Kooy) and 565 m above sea level (Hof, Germany). Data are from  
124 the German Weather Service (DWD) (DWD Climate Data Center (CDC), 2021) and the Royal Dutch  
125 Meteorological Institute (KNMI) (KNMI, 2021). Both weather services provide open-access climate data  
126 including but not limited to precipitation, wind speed, relative humidity, maximum and minimum  
127 temperature. Also incoming shortwave radiation is needed as forcing variable for the HYDRUS-1D version  
128 4.17 model. The KNMI provides daily incoming shortwave radiation data for most of the meteorological  
129 sites since the 1960s. The radiation data are also available for the DWD stations but for shorter time  
130 periods and only for a few stations long term measurements are available. In this study, incoming  
131 shortwave radiation was used in the simulations for the Dutch sites. For German sites, sunshine duration  
132 was used to estimate incoming shortwave radiation according to the equation:

133 
$$R_s = (1 - \alpha) \left( a_s + b_s \frac{n}{N} \right) R_a \quad (1)$$

134 where  $R_s$  is incoming shortwave radiation [ $\text{MJ m}^{-2}\text{d}^{-1}$ ],  $R_a$  is extraterrestrial radiation [ $\text{MJ m}^{-2}\text{d}^{-1}$ ],  $\alpha$  is the  
135 albedo or the canopy reflection coefficient (i.e., 0.23 for grassland),  $a_s$  and  $b_s$  are parameters for the  
136 fraction of radiation (i.e.,  $a_s = 0.25$ ,  $b_s = 0.5$ ),  $n/N$  is the relative sunshine fraction [-], in which  $n$  is the  
137 number of measured sunshine hours and  $N$  is the maximum possible number of sunshine hours for the  
138 specific day of the year.



139

140 **Figure 1.** The 31 climatic stations used in this study, situated across Germany (26) and Netherlands (5)  
 141 (data downloaded from DIVA-GIS [<https://www.diva-gis.org/>])

142 The four drought indices and drought events were calculated relative to a reference period of 55 years  
 143 (1965 to 2019). This period has been selected so that a large number of stations could be considered for a  
 144 relatively long period. However, not all stations provide complete datasets and some minor gaps exist in  
 145 the datasets. The gaps were filled by a linear regression equation that was fitted using data from a  
 146 neighboring station. Table 2 presents the neighboring stations used to fill data gaps by regression.  
 147 Meteorological stations which are not listed in Table 2 do not have missing data.

148 **Table 2.** Meteorological stations and their neighboring stations, used to fill data gaps by linear regression

Stations with gaps	Regression stations
Aachen	Köln-Bonn
Artern	Augsburg
Augsburg	Artern
Bremen	Bremerhaven
Bremerhaven	Bremen
Chemnitz	Hof
Essen	Köln-Bonn
Freiburg	Konstanz
Gießen-Wettenberg	Frankfurt-Main
Hamburg-Fuhlsbüttel	Soltau
Hannover	Soltau
Helgoland	List auf Sylt
Hof	Chemnitz
Köln-Bonn	Aachen
Lindenberg	Potsdam



List auf Sylt	Helgoland
Magdeburg	Gardelegen
Nürnberg	Regensburg
Öhringen	Freiburg
Potsdam	Lindenberg
Regensburg	Nürnberg
Rostock-Warnemünde	Schwerin
Saarbrücken-Ensheim	Trier-Petrisberg
Schwerin	Rostock-Warnemünde
Soltau	Bremen
Trier-Petrisberg	Saarbrücken-Ensheim
De Kooy	De Bilt
Eelde	De Bilt
Vlissingen	De Bilt

149

## 150 2.2 Methods

### 151 2.2.1 HYDRUS 1-D simulations

152 Various models have been used to assess droughts (Mishra and Singh, 2011). In this study, the HYDRUS-  
 153 1D version 4.17 model (Simunek et al., 2005; Šimůnek et al., 2008; Huang et al., 2020) was applied to  
 154 calculate actual ET, soil moisture and resulting drought statistics. We simulated uniform water flow in 2  
 155 meters deep soil columns with homogeneous soil texture and a root uptake sink term.

156 All simulations are done for pasture with a rooting depth of 50cm. Flow for the 2m soil column is simulated  
 157 with the modified Richards equation:

$$158 \quad \frac{\partial \theta}{\partial t} = \frac{\partial}{\partial z} \left[ K(\theta) \left( \frac{\partial h}{\partial z} + 1 \right) \right] - S + P - ET \quad (2)$$

159 where  $\theta$  is volumetric water content [ $L^3L^{-3}$ ],  $t$  is time [T],  $z$  is depth along the soil profile [L],  $h$  is pressure  
 160 head [L],  $S$  is source/sink term [ $T^{-1}$ ],  $P$  is precipitation [ $T^{-1}$ ],  $ET$  is actual ET [ $T^{-1}$ ], and  $K(\theta)$  is the unsaturated  
 161 hydraulic conductivity function [ $LT^{-1}$ ]:

$$162 \quad K(\theta) = K_s K_r(\theta) \quad (3)$$

163 where  $K_s$  is saturated hydraulic conductivity [ $LT^{-1}$ ] and  $K_r$  the relative hydraulic conductivity [ $LT^{-1}$ ]. The sink  
 164 term is the transpiration of the pasture here.  $K_r$  is a function of soil moisture content (Van Genuchten,  
 165 1980):

$$166 \quad K_r(\theta) = \theta^{1/2} [1 - (1 - \theta^{1/m})^m]^2 \quad (4)$$

167 Unsaturated soil hydraulic properties were determined using the Van Genuchten model (Van Genuchten,  
 168 1980) with a fixed air-entry value of  $-2$ cm in order to achieve better outcomes for finer soils:

$$169 \quad \theta(h) = \begin{cases} \theta_r + \frac{\theta_s - \theta_r}{[1 + |\alpha h|^n]^m}, & h < 0 \\ \theta_s, & h > 0 \end{cases} \quad (5)$$



170 
$$m = 1 - \frac{1}{n}, n > 1 \tag{6}$$

171 where  $\alpha$  [ $L^{-1}$ ] and  $n$  are the inverse of the air-entry value and the pore-size distribution index respectively,  
172  $\theta_s$  is saturated soil water content and  $\theta_r$  is residual soil water content. The lower boundary is a free  
173 drainage boundary condition and the upper boundary is governed by atmospheric conditions without  
174 surface runoff and ponding. The potential ET was calculated using the Penman-Monteith equation (Allen  
175 et al., 1998) with the assumption of a pasture height of 12 cm, an albedo of 0.23, a LAI of 2.0 and a rooting  
176 depth of 50 cm. Alternatively, simulations were also performed with a higher LAI-value of 2.88, to  
177 investigate the impact of LAI on the results.

178  
179 The models were run for five soil types (clay, silt, loam, loamy sand and sandy loam) in order to see the  
180 impact of soil type on the drought indices. The soil hydraulic properties were determined from texture  
181 according to Carsel and Parrish (1988), see also Table 3.

182

183 **Table 3.** Soil hydraulic parameter values for the selected texture types in the simulations

Parameters	Clay	Silt	Loam	Sandy loam	Loamy sand
$K_s$ , cm d <sup>-1</sup>	4.8	6	24.96	106.1	350.2
$\alpha$ , cm <sup>-1</sup>	0.008	0.016	0.036	0.075	0.124
$n$	1.09	1.37	1.56	1.89	2.28
$\theta_s$	0.38	0.46	0.43	0.41	0.41
$\theta_r$	0.068	0.034	0.078	0.065	0.057

184

185 We monitored soil moisture in the simulated soil columns at five different soil depths and calculated  
186 average soil water content on the basis of these five values. These monitoring schemes differed slightly  
187 between soil types. For the fine soils (clay, silt and loam) the vertical discretization was 2.5mm and  
188 monitoring nodes were inserted at 4.75 cm, 15.5 cm, 25.25 cm, 35.25 cm and 45.25 cm, covering the root  
189 zone of 50cm. For the coarse soils (sandy loam and loamy sand) the vertical discretization was 2.0mm and  
190 monitoring nodes were inserted at 4.8 cm, 15 cm, 25 cm, 35cm and 51cm depth.

### 191 2.2.2 Drought indices

192 Due to the complex nature of droughts, one single drought index is not sufficient for drought detection  
193 (Hao and AghaKouchak, 2014). In this study, we focus on meteorological drought and agricultural drought.  
194 In this context, four drought indices are evaluated.

#### 195 2.2.2.1 The Standardized Precipitation Index (SPI)

196 The SPI was developed by (McKee et al., 1993) and is calculated based on long-term precipitation data  
197 (minimum 30 years). A time series of precipitation data is transformed to a normal distribution after  
198 fitting to a probability distribution (McKee et al., 1993), which allows for estimation of dry and wet  
199 periods. Positive SPI values greater than median precipitation means wetter conditions than normal. The



200 SPI can be calculated for different time scales (i.e. 3, 6, 9, 12 and 24 months) and can be calculated as  
201 follows:

$$202 \quad \text{SPI}_{i,j} = \frac{P_{i,j} - \bar{P}_j}{\sigma_{P,j}} \quad (7)$$

203 where  $P_{i,j}$  [mm] is the precipitation for time interval  $j$  (6 months or 12 months in this study) of the year  $i$ ,  
204  $\bar{P}_j$  [mm] is the average precipitation over the studied period and  $\sigma_{P,j}$  [mm] is the standard deviation of  
205 precipitation for time interval  $j$  over the studied period (Cavus and Aksoy, 2019; Fathian et al., 2021).  
206 Extreme droughts are characterized by negative SPI values, see Table 4. SPI is one of the most used  
207 drought indices (Mishra and Singh, 2010; Gudmundsson and Seneviratne, 2015; Zink et al., 2016). It is  
208 also a drought index recommended by the World Meteorological Organization (WMO) and German  
209 Weather Service (DWD). Compared to another widely used drought index, the Palmer drought severity  
210 index (PDSI) (Palmer, 1965), SPI has the advantage of simplicity because it only requires information on  
211 precipitation. SPI has limitations for shorter time series and dry climates, but in this study long time  
212 series of 55 years (1965 – 2019) are calculated and the climate over the study domain is in general  
213 temperate humid, although drier in Eastern Germany. The severity of droughts over the simulation time  
214 period has been assessed for the summer period from April to September (SPI-6), as well as for periods  
215 of 12 months (SPI-12). Droughts are classified into four classes, ranging from mild droughts to extreme  
216 droughts (McKee et al., 1993). See also Table 4.

217

**Table 4.** Classification of SPI

SPI-values	Drought classification
Between -0.99 and 0	Mild drought
Between -1.49 and -1.00	Moderate drought
Between -1.99 and -1.50	Severe drought
Less than – 2.00	Extreme drought

218

#### 219 **2.2.2.2 Standardized Soil Moisture Index (SSI)**

220 Similar to SPI, SSI is also calculated by deriving probabilities from soil moisture time series (AghaKouchak,  
221 2014; Hao and AghaKouchak, 2014), which allows to determine periods with negative and positive soil  
222 moisture anomalies. SSI is calculated in this work for two time intervals, SSI-6 for summer droughts (April-  
223 September) and SSI-12 for annual droughts. SSI is therefore determined using the same principles as SPI.  
224 Therefore, the SSI can be calculated as follows:

$$225 \quad \text{SSI}_{i,j} = \frac{\theta_{i,j} - \bar{\theta}_j}{\sigma_{\theta,j}} \quad (8)$$

226 Where  $\theta_{i,j}$  [mm] is the soil moisture content for time interval  $j$  (6 months or 12 months in this study) of  
227 the year  $i$ ,  $\bar{\theta}_j$  [mm] is the average soil moisture content over the studied period and  $\sigma_{\theta,j}$  [mm] is the  
228 standard deviation of soil moisture content for time interval  $j$  over the studied period.





### 229 2.2.2.3 Potential Precipitation Deficit (PPD)

230 Potential precipitation deficit is a drought index developed by the Royal Dutch Meteorological Institute  
231 (KNMI) to assess drought events and it is defined by the difference between potential ET and precipitation.  
232 PPD also stands for meteorological drought but in addition to SPI, PPD includes information on the  
233 atmospheric evapotranspiration demand. Specific for the conditions in the Netherlands and Germany, the  
234 deficit is calculated for the period between April and September with large potential ET. PPD is defined as  
235 the cumulative deficit between potential ET according to the Penman Monteith method and precipitation  
236 and calculated for each day in the period between the 1<sup>st</sup> of April and 30<sup>th</sup> of September. Typically, PPD  
237 increases during summer as potential ET is larger than precipitation. PPD cannot become negative (if  
238 cumulative precipitation is larger than cumulative potential ET) and will have as minimum value zero. The  
239 maximum PPD value reached in the period between the 1<sup>st</sup> of April and the 30<sup>th</sup> of September (typically in  
240 August) is recorded.

### 241 2.2.2.4 Evapotranspiration Deficit (ET<sub>def</sub>)

242 A direct indicator for drought stress affecting vegetation is the difference between potential ET and actual  
243 ET. If actual ET is smaller than potential ET, this indicates that not enough soil water was available to satisfy  
244 the atmospheric demand. This also implies that crop yield is affected. We define therefore as further  
245 indicator for drought stress (ET<sub>def</sub>):

$$246 \quad ET_{def} = \sum_{i=1}^n (ET_{pot,i} - ET_{act,i}) \quad (9)$$

247 where ET<sub>pot</sub> is potential ET, ET<sub>act</sub> is actual ET, *i* is a day between the 1<sup>st</sup> of April (*i*=1) and the 30<sup>th</sup> of  
248 September (*i*=183) and *n* is 183 days.

### 249 2.2.3 Trend analysis

250 Trends are analyzed in this study according the Theil-Sen slope (Theil, 1950; Sen, 1968) and the significance  
251 is assessed based on the Mann-Kendall (MK) test with *p* value 0.05, which allows for pre-whitening in order  
252 to eliminate the impact of autocorrelation (Hamed and Rao, 1998; Yue and Wang, 2004). The MK test is  
253 nonparametric and is regularly used in hydrometeorological trend detection and the python package  
254 'pymannkendall' is used for computations.

255

## 256 3 Results

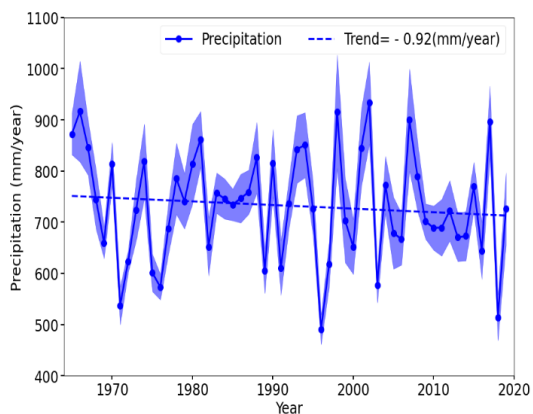
### 257 3.1 Trends of precipitation, potential ET, actual ET, soil moisture and drought indices for 1965-2019

#### 258 3.1.1 Precipitation trends

259 Figure 2 displays trends of precipitation for different regions in Germany and the Netherlands. Coinciding  
260 with Spinoni's study (Spinoni et al., 2015), Fig. 2 shows that precipitation for all four areas of Germany  
261 show decreasing trends, but with clear differences. In southern Germany, the precipitation decrease was  
262 strongest (-2.2 mm/year) while in the East the decreasing trend was only -0.23 mm/year. Different to the  
263 German regions, the Netherlands experienced a small increase in precipitation at the rate of 0.385  
264 mm/year. Spinoni et al. (2015) reported also an increase for the Netherlands, but for the period 1950 –  
265 2012.

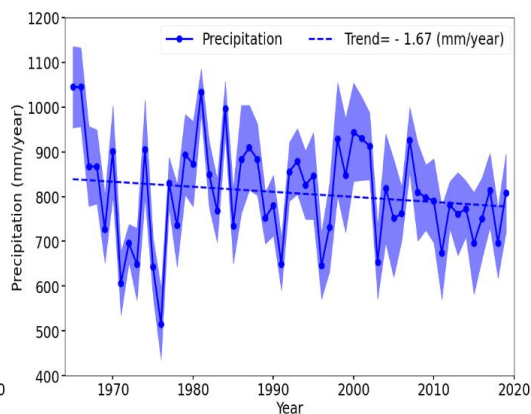


266



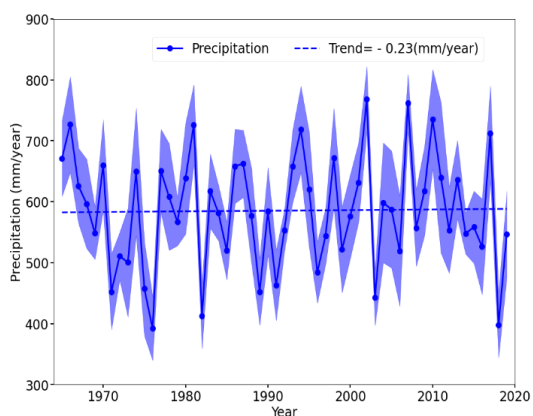
(a)

267



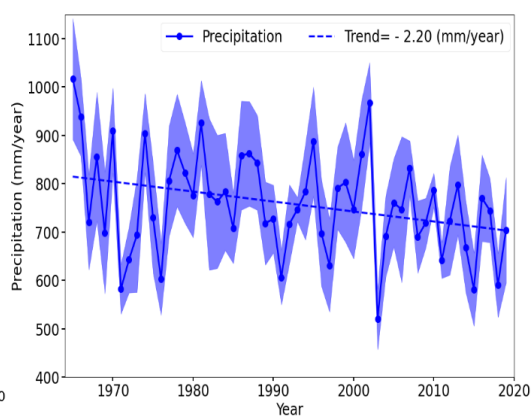
(b)

268



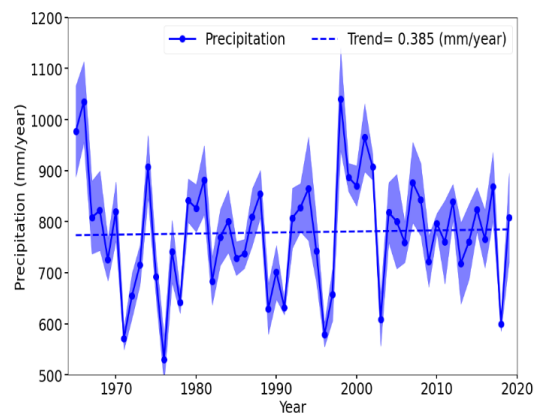
(c)

269



(d)

270



(e)

271



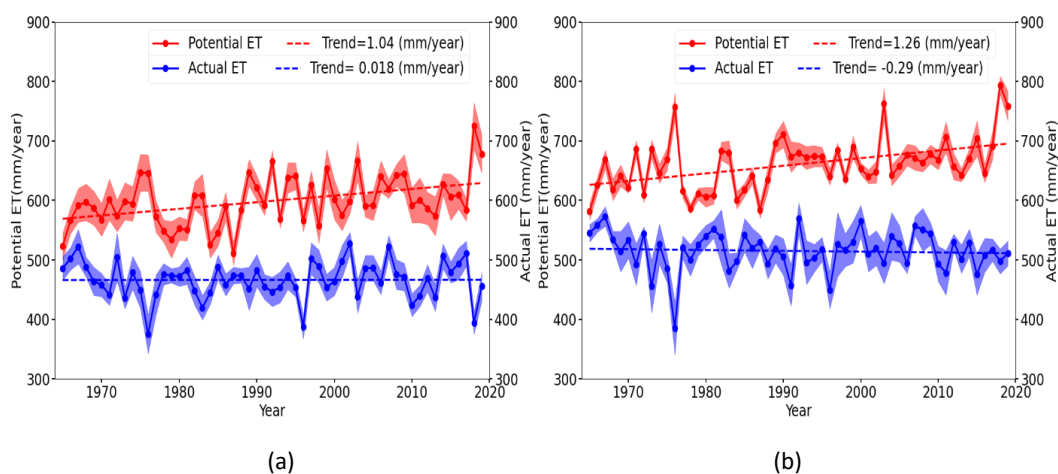
272 **Figure 2.** Precipitation trends in (a) North Germany, (b) West Germany, (c) East Germany, (d) South  
273 Germany and (e) Netherlands. Shaded areas indicate the 95% confidence interval estimated from (the  
274 limited) number of sites in each domain.

### 275 3.1.2 Potential ET and actual ET trends

276 Figure 3 shows that potential ET has increased in all areas, with trends varying between 1.04 mm/year  
277 (northern Germany) and 1.66 mm/year (Netherlands). Table 5 also shows the potential ET trends, and  
278 indicates that for all five regions considered here the trend of increasing potential ET is significant  
279 (coinciding with Spinino et al. (2015)). However, actual ET trends show different trend signs (Fig. 3), with  
280 increasing trends for Northern Germany, Eastern Germany and Netherlands and decreasing trends for  
281 Western Germany and Southern Germany. The decreasing trends in the West and South of Germany can  
282 be related to strong decreasing precipitation trends in those two domains.

283

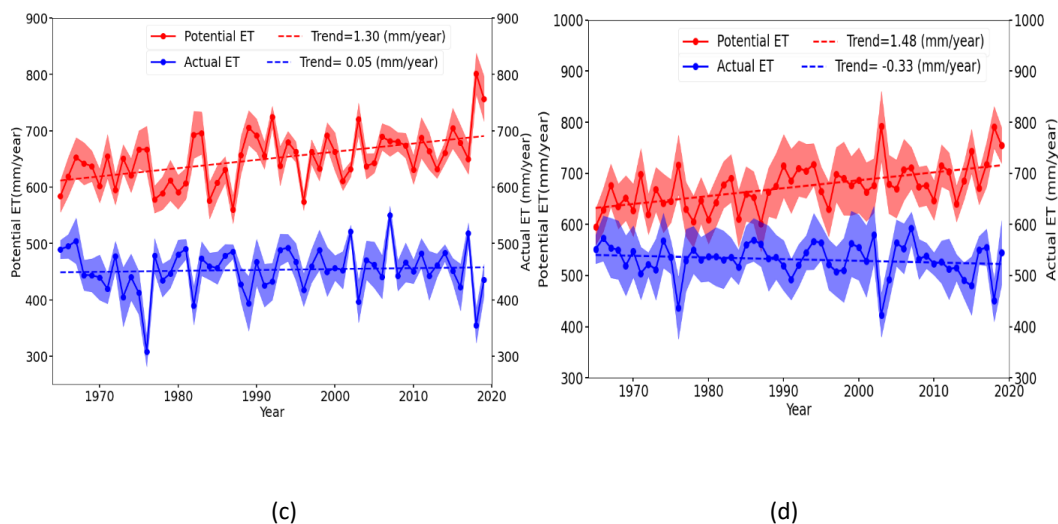
284

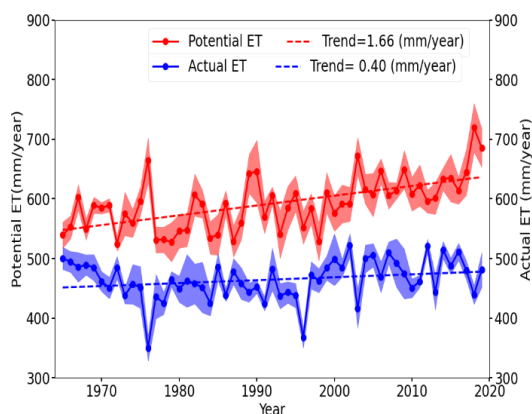


285

286

287





288

289

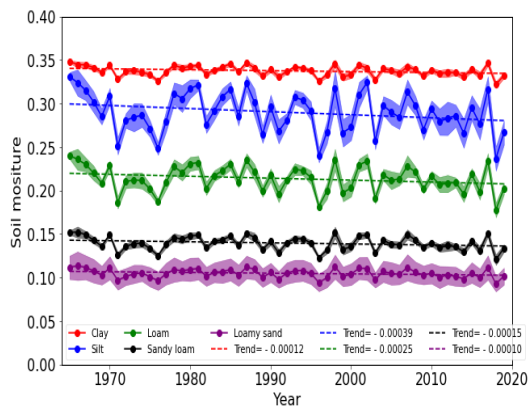
(e)

290 **Figure 3.** Potential ET (red line) and actual ET (blue line) trends in the (a) North, (b) West, (c) East and (d)  
 291 South of Germany and (e) Netherlands. Shaded areas indicate the 95% confidence interval estimated  
 292 from (the limited) number of sites in each domain.

293

294 **3.1.3 Soil moisture trends**

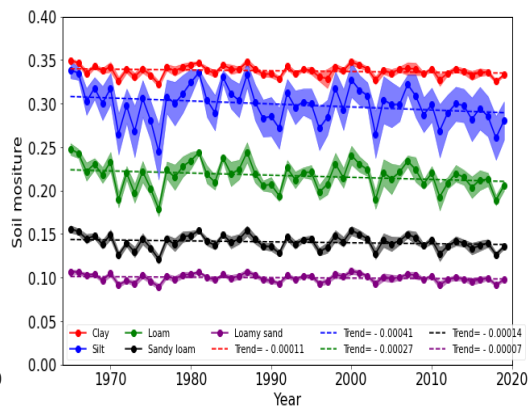
295 Figure 4 displays the temporal trend in the average yearly soil moisture content, for the four German  
 296 domains, the Netherlands and the five different soils. As expected, soil water contents are highest for clay  
 297 and lowest for sandy loam and loamy sand. For all soils a decreasing soil moisture trend can be observed  
 298 over all domains, which is significant for clay and silt, but not significant for all the other soil types. The  
 299 trends are less pronounced for the Netherlands and eastern Germany than for the other three domains.  
 300 For all soil types the year 2018 has the lowest average soil moisture content except for 1976 in western  
 301 Germany and Netherlands. The different soil types show a similar ranking of the different years but  
 302 interannual variability is higher for loam and silt.



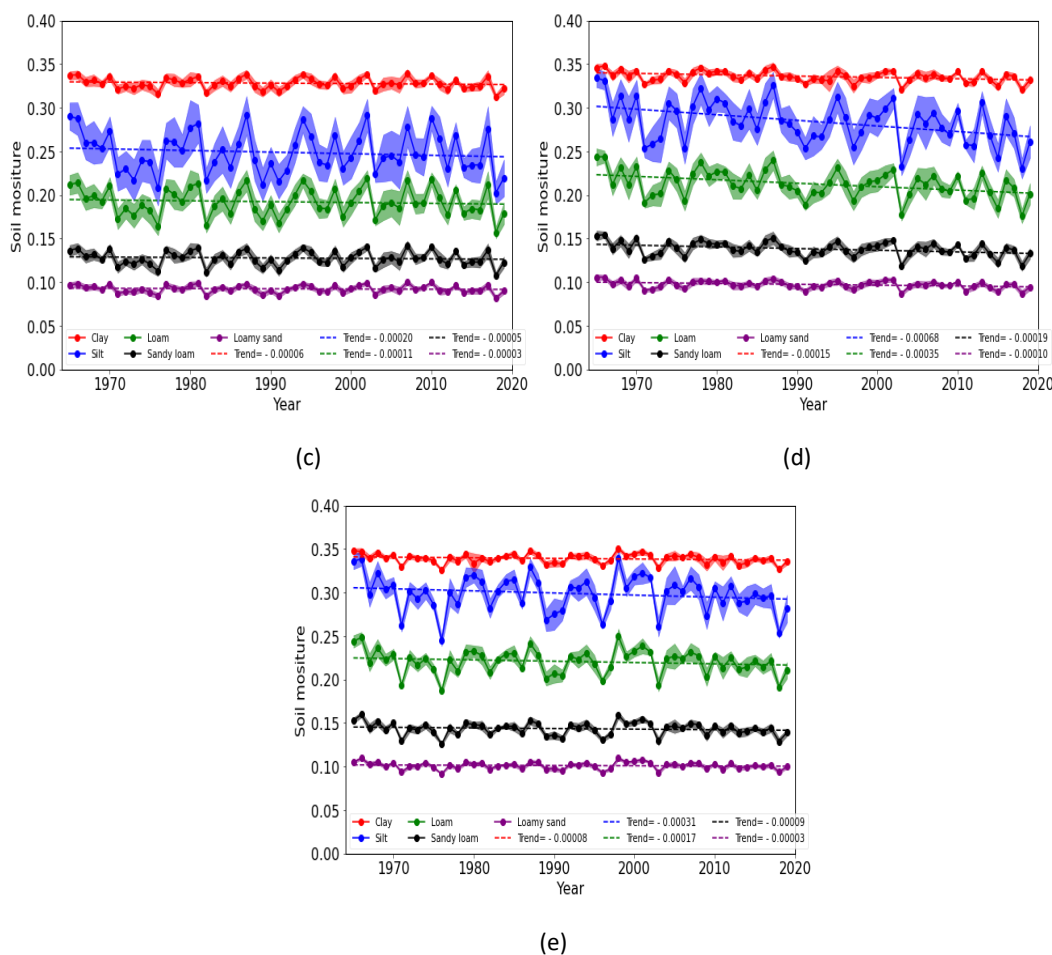
303

304

(a)



(b)



305

306

307

308

309 **Figure 4.** Trends in average yearly soil moisture content for (a) North, (b) West, (c) East and (d) South of  
 310 Germany and (e) the Netherlands, for five different soil textures (clay (red), silt (blue), loam (green),  
 311 sandy loam (black) and purple (loamy sand)). The trend coefficients are also indicated in each of the  
 312 figures. Shaded areas indicate the 95% confidence interval estimated from (the limited) number of sites  
 313 in each domain.

314

315 Table 5 shows the trends in potential ET, actual ET and soil moisture content simulated by HYDRUS-1D  
 316 version 4.17, for the different regions in Germany and the Netherlands. Actual ET shows a non-significant  
 317 decreasing trend in western and southern Germany which can be explained by decreasing precipitation.  
 318 The Netherlands shows the strongest increase in actual ET, which can be explained by the increasing  
 319 precipitation and potential ET trends. In northern and eastern Germany, the actual ET trends show a slight  
 320 non-significant increase, in spite of the decreasing precipitation trend, which can be explained by the fact  
 321 that actual ET is often energy limited, and not moisture limited. Root zone soil moisture content as  
 322 simulated by HYDRUS shows over all regions a non-significant decreasing trend, except for southern



323 Germany where the trend is significant. The decreasing trends can be explained by a combination of  
324 decreasing precipitation (in most regions) and increasing potential ET.

325

326 **Table 5.** Trends for potential ET, actual ET and soil moisture for the different studied regions in Germany  
327 and the Netherlands over the period 1965-2019

Regions	Potential ET (mm/year)	Significance	Actual ET (mm/year)	Significance	Soil moisture (10 <sup>-3</sup> m <sup>3</sup> m <sup>-3</sup> )	Significance
Germany-East	+1.30	yes	+0.05	no	-0.09	no
Germany-West	+1.25	yes	-0.28	no	-0.21	no
Germany-North	+1.04	yes	+0.018	no	-0.20	no
Germany-South	+1.48	yes	-0.33	no	-0.29	yes
Netherlands	+1.66	yes	+0.40	no	-0.13	no

328

### 329 3.1.4 Temporal trends of SPI, SSI, PPD and ET deficit

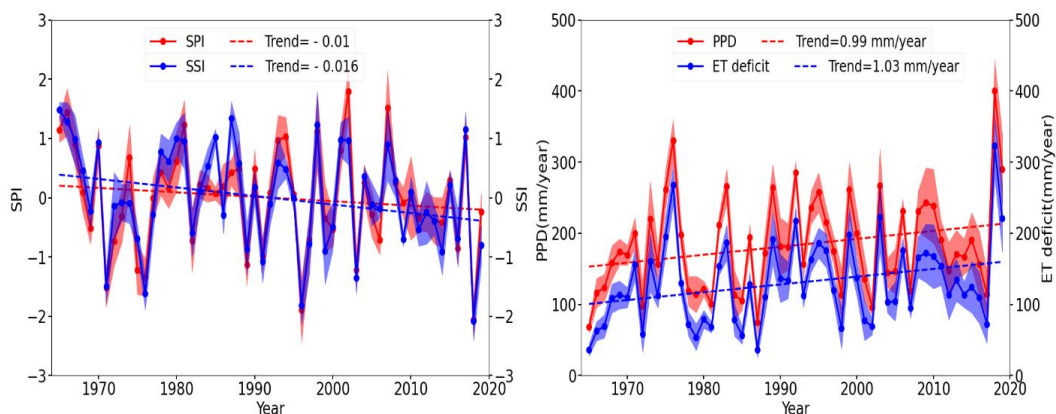
330 The four drought indices, determined for the 31 meteorological stations, were averaged for the five  
331 domains and the yearly values and trends are displayed in Figs. 5 and 6. The SPI shows decreasing trends  
332 over all four German regions, which is indicative of increased frequency of meteorological drought  
333 conditions. The decreasing trend is strongest over southern and western Germany, and only significant for  
334 southern Germany. On the contrary, for the Netherlands an increasing trend can be observed. All five  
335 regions show a decreasing SSI-trend, in this case also the Netherlands. The negative trends indicate  
336 increasing frequency of agricultural droughts. For all five regions the slope of the SSI-regression line is  
337 more negative than the slope of the SPI-regression line, which indicates that the frequency and/or  
338 intensity of agricultural droughts is increasing faster than the frequency and/or intensity of meteorological  
339 droughts. This indicates that besides a decrease in precipitation, there are factors which enhance  
340 agricultural droughts. Earlier we saw that for all regions in Germany and the Netherlands a significant  
341 increase of potential ET over the period 1965-2019 was detected. The negative SSI-trends are strongest  
342 for southern and western Germany.

343 The potential precipitation deficit (PPD) and ET deficit show positive trends for all five regions, pointing  
344 towards more agricultural drought, as water is lacking to fulfill the potential evapotranspiration demand.  
345 In western and southern Germany PPD and ET deficit show trends between 1.5 and 1.7 mm/year, which  
346 is larger than for the Netherlands, northern and eastern Germany (1.0-1.2 mm/year). This is related to the  
347 strong and significant increase of potential ET over time, in combination with only small changes in  
348 precipitation amount. The trends are in all cases significant, except PPD in northern and eastern Germany.





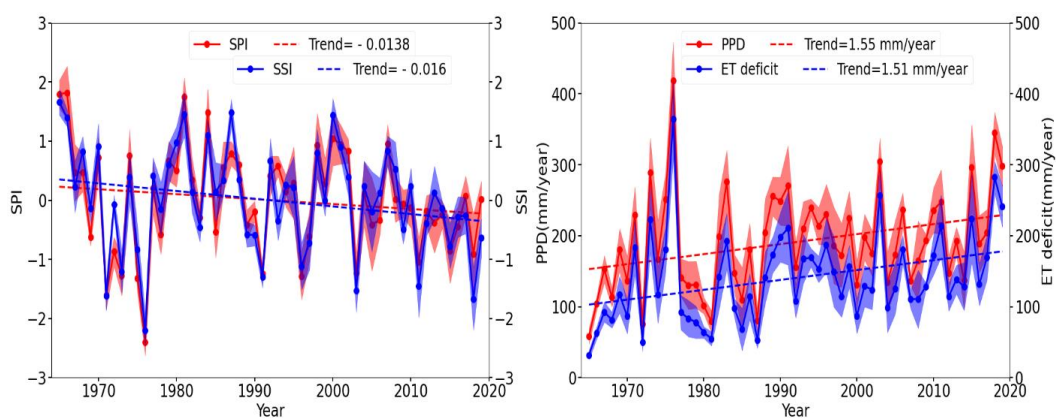
349



350

(a)

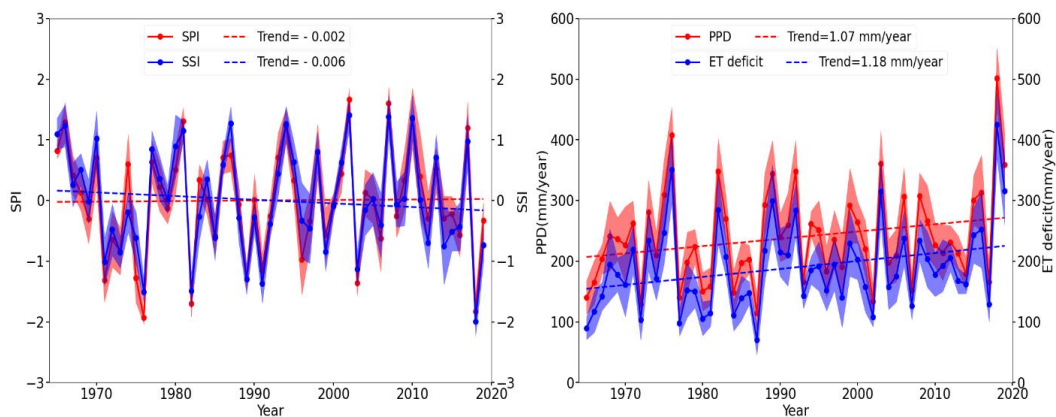
351



352

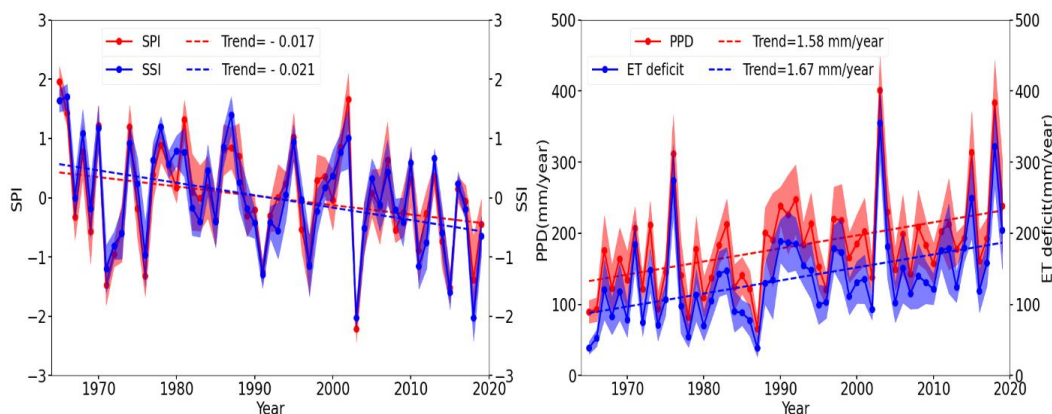
(b)

353



354

(c)

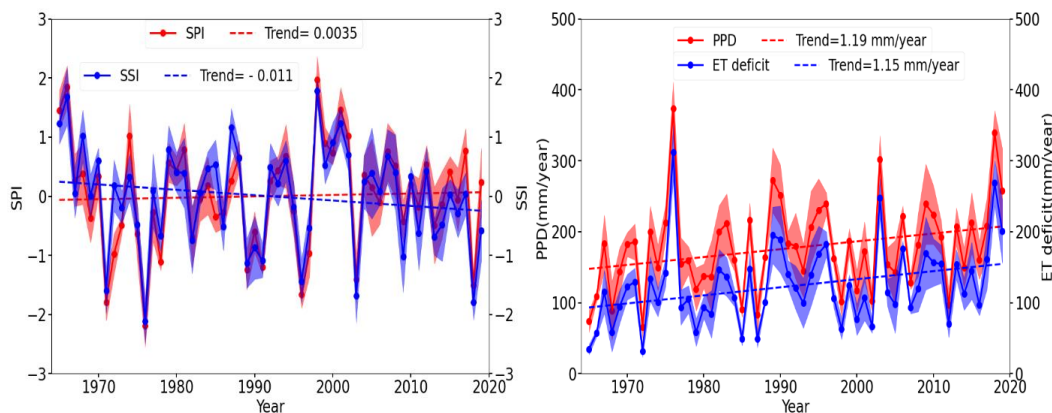


355

356

(d)

357 **Figure 5.** Temporal trends (1965-2019) for SPI and SSI (left), and PPD and ET deficit (right) in (a) northern  
 358 Germany, (b) western Germany, (c) eastern Germany and (d) southern Germany. Shaded areas indicate  
 359 the 95% confidence interval estimated from (the limited) number of sites in each domain.



360

361

(e)

362 **Figure 6.** Temporal trends (1965-2019) for SPI and SSI (left), and PPD and ET deficit (right) over the  
 363 Netherlands. Shaded areas indicate the 95% confidence interval estimated from (the limited) number of  
 364 sites in each domain.

365

366 We analyze now the SPI, SSI, PPD and ET deficit trends for the 31 individual stations. Table 6 summarizes  
 367 results from a trend analysis of the drought indices for the summer period from the 1<sup>st</sup> of April until the  
 368 30<sup>th</sup> of September. The SPI-6 decreased for 23 out of 31 stations (and increased for the other 8 stations)  
 369 with a mean trend of  $-0.071 \text{ decade}^{-1}$  averaged over all 31 stations, only for 4 stations this decrease was  
 370 significant ( $p < 0.05$ ). Results are very similar for SPI-12, but for two more sites the decreasing trend was  
 371 significant. Gudmundsson and Seneviratne (2015) also calculated SPI-12 at the scale of Europe but their  
 372 results were not provided for individual countries or regions. They detected non-significant trends of  
 373 different signs over Germany.





374 Summer soil moisture drought, as evaluated by SSI-6, shows a clear trend of  $-0.186 \text{ decade}^{-1}$  averaged over  
 375 all 31 stations. All stations show a negative trend, and for 17 of these stations there is a significant negative  
 376 trend. On the other hand, soil moisture droughts at the yearly time scale, as evaluated by SSI-12, do not  
 377 show such a pronounced negative trend and only for 8 stations a significant negative trend is found. For 7  
 378 stations even a trend towards increased SSI-12 values is observed. Five of these seven stations are located  
 379 in the Netherlands, again indicating that the Netherlands is less impacted by a trend towards increasing  
 380 droughts than Germany.

381 Finally, both PPD and ET deficit show positive trends indicating increased droughts with an increase of PPD  
 382 of  $1.25 \text{ mm/year}$  and increase of ET deficit of  $1.30 \text{ mm/year}$  averaged over all stations. For PPD 15 of the  
 383 stations and for ET deficit 20 of the stations show significant trends ( $p < 0.05$ ).

384 In summary, the increase of droughts is mainly related to increasing soil moisture deficits, and reduction  
 385 in actual ET. The main driver is not a precipitation decrease, but an increase of potential ET.

386

387 **Table 6.** Number of stations with increasing drought trends and in brackets the number of significant  
 388 drought trends. The mean trend is also given.

Drought indices	SPI-6	SPI-12	SSI-6	SSI-12	PPD (mm)	ET deficit (mm)
Numbers of sites	23 (4)	22 (6)	31 (17)	24 (8)	31 (15)	31 (20)
Mean trend ( $\text{year}^{-1}$ )	-0.0071	-0.0068	-0.0186	-0.0004	1.25	1.30

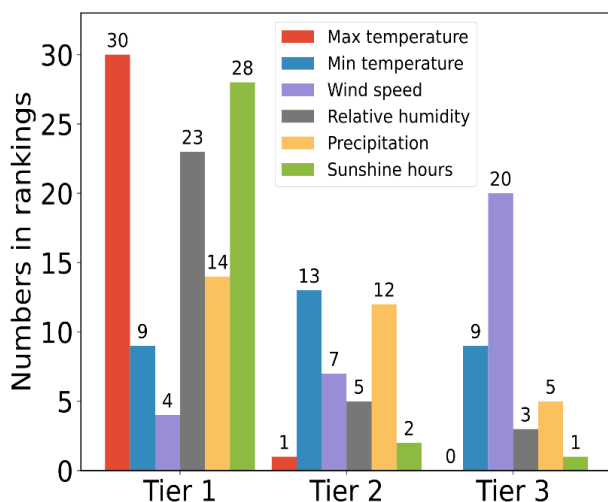
389

390

### 391 3.2 The year 2018 and other drought years during 1965-2019

#### 392 3.2.1 Climatological variables for 2018 in a historical perspective

393 We ranked the position of the year 2018 in the time series of 1965-2019 for six climatic variables and for  
 394 all 31 meteorological stations. Figure 7 shows for each of the six variables for how many of the 31  
 395 meteorological stations 2018 ranked in the top three (Tier 1), in the top ten but not in the top three (Tier  
 396 2), and outside the top ten (Tier 3). Top-ranking implies that meteorological variables were prone to result  
 397 in drought conditions: high temperatures, high incoming shortwave radiation, low precipitation, low  
 398 relative humidity and high wind speed. Figure 7 shows that for 30 out of 31 stations the average maximum  
 399 temperature for 2018 ranks in the top three. Also the total amount of sunshine hours was very high for  
 400 2018 with a top three position for 28 out of 31 stations. Rankings are less pronounced for low relative  
 401 humidity (top three for 23 out of 31 stations), low precipitation (for 14 out of 31 stations in the top three  
 402 of driest years). For daily average minimum temperature, the year 2018 showed less extreme rankings  
 403 (but often in top ten), and wind speed deviated for most stations not much from a normal year (outside  
 404 top ten).



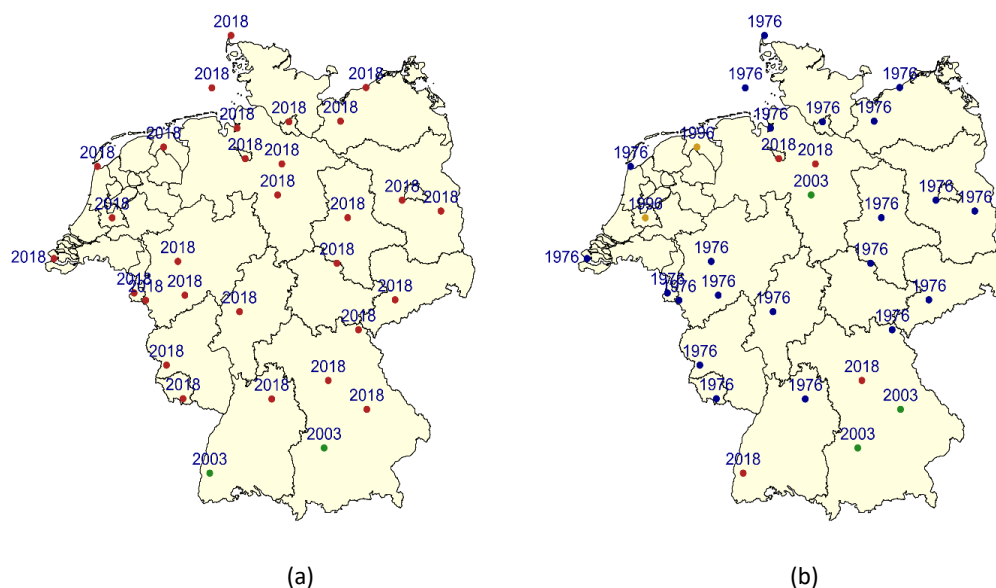
405

406 **Figure 7.** Ranking of climatic variables for the year 2018 in the time series of 1965-2019 (Tier 1=Ranks 1-  
 407 3, Tier 2=ranks 4-10 and Tier 3 =ranks 11-31)

408

### 409 3.2.2 Potential ET and actual ET extremes

410 Figure 8 displays the years with the highest potential ET and the lowest actual ET for the 31 meteorological  
 411 stations. Except two stations in southern Germany (Augsburg and Freiburg), 2018 is the year with the  
 412 highest potential ET. Augsburg and Freiburg had in 2003 the highest potential ET. The summer of 2003 was  
 413 extremely warm over Central Europe (especially Southern Germany, Eastern France, Switzerland and  
 414 Austria). Regarding actual ET, at some meteorological stations (according calculations with HYDRUS-1D  
 415 version 4.17) 2018 had the lowest total sum of actual ET over the complete time series from 1965-2019,  
 416 this is the case for four sites across Germany. However, the year 1976 with the historic summer drought  
 417 had for many meteorological stations the lowest actual ET, due to a combination of low precipitation and  
 418 high atmospheric evaporative demand. This was especially the case for northern and central Germany.  
 419 Three sites in Germany had the lowest calculated actual ET in 2003 and two Dutch stations (Eelde and De  
 420 Bilt) had the lowest calculated actual ET in 1996, which was related to a combination of a relatively limited  
 421 potential ET and drought.



422

423

424 **Figure 8.** The years with the (a) highest potential ET according Penman-Monteith and (b) lowest  
425 actual ET (HYDRUS-calculations) at the different 31 meteorological stations across the Netherlands  
426 and Germany (data downloaded from DIVA-GIS [<https://www.diva-gis.org/>])

427

### 428 3.2.3 The most extreme drought events based on drought indices

429 Figure 9 shows the year with the lowest SPI (precipitation deficit), the lowest SSI (soil moisture deficit), the  
430 largest potential precipitation deficit and the largest ET deficit. The years 1976, 2003 and 2018, all of them  
431 with very warm and dry summers, are most prominent on the maps. For SPI, the year 1976 dominates  
432 over the southern Netherlands and parts of western Germany, 2003 over southern Germany and 2018  
433 over other parts of Germany. For SPI, also other years like 1971 and 1996 appear on the map. It indicates  
434 that meteorological droughts are spatially variable over the past 55 years. For SSI, the spatial patterns are  
435 not very different from SPI but 2018 is at more stations the year that results in the lowest SSI. If we analyze  
436 now the years with the most extreme PPD and ET deficits, nearly exclusively 1976, 2003 and 2018 are the  
437 extreme years. One exception is the 1989 drought in the state Saxony-Anhalt in Germany. The year 2003  
438 has in general the highest PPD and ET deficits in southern Germany, the year 1976 in the Netherlands and  
439 western Germany and the year 2018 in northern and eastern Germany. In summary, the drought event  
440 2018 impacted especially northern and eastern Germany and is characterized by very high potential ET  
441 (besides lower precipitation), while the 1976 drought is in general characterized by high potential ET (but  
442 not as high as in 2018) and very low precipitation (often lower than in 2018).





456 drought indices which include potential ET (PPD and ET deficit), the summer of 2018 ranks first and before  
457 1976 and 2003; 2018 is more extreme than 1976 (2<sup>nd</sup>) and 2003 (3<sup>rd</sup>). These indices show again that the  
458 2018 drought was extreme, especially related to the very high potential ET and the lack of water for plant  
459 transpiration.

460

461 **Table 7.** Drought severity in 2018 in comparison with 1976 and 2003. The most extreme values are  
462 printed bold italic.

Year	SPI-6	SPI-12	SSI-6	SSI-12	PPD (mm)	ET deficit (mm)
2018	-1.71	-1.56	-1.60	<b>-1.92</b>	<b>399.6</b>	<b>329.2</b>
2003	-1.22	-1.47	-1.62	-1.52	327.0	279.8
1976	<b>-2.11</b>	<b>-1.81</b>	<b>-1.87</b>	-1.66	368.4	313.9

### 463 3.3 Simulations for different LAI

464 Alternatively, we performed simulations with a higher LAI-value equal to 2.88, to investigate the impact  
465 on the results. Potential ET is strongly related to LAI, and is larger for higher LAI. Figure S1 (supplementary  
466 material) shows that potential ET is always considerably larger for a LAI of 2.88 compared to a LAI of 2.0,  
467 50 to 100mm on year basis, and also the trends are slightly stronger.

468 Although LAI impacts potential (and actual) ET, its impact on yearly average soil moisture content is limited,  
469 and simulated soil moisture contents for LAI equal to 2.88 are only very slightly smaller than soil moisture  
470 contents for LAI equal to 2.0. The soil moisture trends are also nearly identical for the two different LAI-  
471 values. Plots are shown in the supplementary material (Fig. S2).

472 Figures S3 (supplementary material) and S4 (supplementary material) show the PPD and ET-deficit trends  
473 for the different regions and for the two different LAI-values. The figures illustrate that LAI=2.88 results in  
474 higher PPD and higher ET-deficit than LAI=2.0. For PPD, the largest differences between the temporal  
475 trends for LAI=2.0 and LAI=2.88 are simulated for northern Germany where the PPD-trend is 0.99 mm/year  
476 for LAI=2.0 and 1.36 mm/year for LAI=2.88. For ET-deficit, western Germany, southern Germany and  
477 northern Germany show the largest increase in the slope of the trend line, comparing LAI=2.88 and LAI=2.0.  
478 However, the overall picture is the same for LAI=2.0 and LAI=2.88, and the main difference is the  
479 magnitude of PPD and ET-deficit.

## 480 4 Discussion

481 This study was carried out for pasture, and we investigated also the impact of different LAI-values on the  
482 simulated temporal trends in drought indices. However, for other vegetation types with deeper roots and  
483 higher LAI, the temporal trends and rankings we found here could be different. It can be expected that  
484 deeper rooting vegetation like forests can take up water from deeper soil layers so that forests are not  
485 affected so fast by droughts as crops or pasture (Kleine et al., 2020). As a consequence, the ET-deficit might  
486 show a less pronounced temporal trend for forests. It is expected that the other drought indices (SPI, SSI,  
487 PPD) for forests are quite similar to grassland.



488 In our simulations, we used a free drainage lower boundary condition. Alternatively, the lower boundary  
489 condition could be a groundwater table, whose level typically also varies over time and is lower during  
490 summer time and shallower during winter time. The simulated temporal trends of drought indices could  
491 be affected by the lower boundary condition, as groundwater affects soil moisture contents and actual  
492 evapotranspiration. During drought conditions, it can provide an additional water source for the  
493 vegetation and buffer droughts, resulting in a smaller ET-deficit. The presence of a shallow groundwater  
494 body can therefore also affect the ranking of the most extreme drought years. For example, if a drought  
495 year is preceded by a wet winter which resulted in relatively high groundwater tables at the beginning of  
496 the summer season, the summer drought can be buffered by the relatively high groundwater tables,  
497 reducing the ET-deficit compared to a situation with deeper groundwater tables. A further limitation is  
498 that we assumed a no ponding condition at the land surface. This assumption can also affect the simulated  
499 removal of water from the soil column, soil moisture contents and actual evapotranspiration.

500

## 501 **5 Conclusions**

502 We analyzed meteorological, soil moisture and agricultural droughts over Germany and the Netherlands  
503 for the period 1965-2019 with separate analysis for four different German regions (north, west, east and  
504 south). It was evaluated how exceptional the 2018 drought was. Simulations were done for 31 locations  
505 distributed over Germany and the Netherlands with long meteorological time series to drive the HYDRUS-  
506 1D model for unsaturated flow in soils. Simulations were done for five different soil types at each location  
507 and for pasture with two different LAI-values. The main conclusions are:

- 508 1. The year 2018 experienced very high maximum temperatures, very high sunshine duration, and  
509 low relative humidity across the study domain, and was for most studied sites the year with the  
510 highest potential ET. In terms of precipitation deficit, 2018 was for many locations not exceptional  
511 and only for 8 locations (out of 31) the standardized precipitation index (SPI) had in 2018 the  
512 lowest value in the time series of 1965-2019. The years 1976 (especially in the Netherlands and  
513 western Germany) and 2003 (especially in southern Germany) were often drier in terms of SPI.  
514 The year 2018 was more exceptional in terms of soil moisture drought and for 13 out of 31 stations  
515 SSI (standardized soil moisture index) was in 2018 the lowest in the time series of 55 years. This  
516 was especially the case for northern and eastern Germany. The year 2018 was remarkable in terms  
517 of potential precipitation deficit (PPD, precipitation minus potential ET) and evapotranspiration  
518 deficit (accumulated difference between potential ET and actual ET), related to the very high  
519 potential ET. For half of the stations (especially in northern, central and eastern Germany) 2018  
520 was the most extreme year in the time series since 1965. This illustrates that the 2018 drought  
521 was especially extreme and intensified by the high potential ET, affecting reductions in crop yield  
522 due to the missing water for plant transpiration. Other years with wide spread severe droughts  
523 were especially 1976 and 2003, but in terms of soil moisture drought and ET drought they were  
524 less extreme than 2018 over the study domain.  
525
- 526 2. The trends in the four drought indices over the period 1965-2019 showed that meteorological  
527 droughts (in terms of SPI-6 and SPI-12) increased at many locations, especially in Germany,  
528 whereas at other locations meteorological drought decreased, especially in the Netherlands. Only  
529 at a few locations the trend towards more severe meteorological droughts were significant. Soil  
530 moisture or agricultural drought, as characterized by SSI-6 and SSI-12 increases at most locations,



531 SSI-6 even at all locations. SSI-6 shows a significant trend towards more soil moisture droughts for  
532 slightly more than half of the locations. PPD and ET deficit show even more pronounced trends  
533 with trends towards increased water deficit at all locations, and significant trends for 15 out of 31  
534 (PPD) and 20 out of 31 (ET deficit) locations. Significant trends towards more severe droughts in  
535 terms of SSI, PPD and ET deficit occur in spite of small changes in total precipitation amounts.  
536 These significant trends are driven by increased potential ET (related to higher temperatures,  
537 higher incoming radiation and lower relative humidity) and a shift of precipitation amounts during  
538 the year with increasing precipitation in winter and decreasing precipitation in summer.

539

540 3. Simulations were limited to pasture, a relatively simple representation of vegetation, and a free  
541 drainage boundary condition. It would be of interest to extend the simulations to include different  
542 crop types and natural vegetation, as well as different boundary conditions including  
543 groundwater-controlled systems. We expect for crops similar results as for pasture, but for deep  
544 rooting vegetation and groundwater-controlled systems the ranking of the different drought years  
545 might change, for example if at the beginning of a drought year groundwater levels are relatively  
546 high for the time of year, allowing for an additional water buffer during the dry summer.

547

#### 548 **Data and code availability**

549 The code and datasets relevant to this study can be provided from the corresponding author upon request.

#### 550 **Author contributions**

551 HJHF, YH and JW designed the study. YH (completely) and JW (partially) developed the programming code  
552 and performed the simulations. YH, JW and HJHF analysed and interpreted the results. HJHF and HV  
553 supervised the work. YH prepared the manuscript with contributions from all co-authors.

#### 554 **Competing interests**

555 The authors declare no competing interests.

#### 556 **Acknowledgement**

557 Yafei Huang (No. 201608500073) appreciates financial support from the China Scholarship Council.  
558 Harrie-Jan Hendricks-Franssen kindly acknowledges support from Germany's Excellence Strategy (EXC  
559 2070–390732324, project PhenoRob).

#### 560 **References**

561 AghaKouchak, A.: A baseline probabilistic drought forecasting framework using standardized soil  
562 moisture index: application to the 2012 United States drought, *Hydrology and Earth System Sciences*, 18,  
563 2485, <https://doi.org/10.5194/hess-18-2485-2014>, 2014.

564 Allen, R. G., Pereira, L. S., Raes, D., and Smith, M.: *Crop evapotranspiration-Guidelines for computing*  
565 *crop water requirements (FAO Irrigation and drainage paper 56)*, Rome: FAO, 300, D05109, 1998.





- 566 AMS: Statement on meteorological drought, *Bulletin of the American Meteorological Society*, 85, 771-  
567 773, 2004.
- 568 Anderson, M. C., Zolin, C. A., Sentelhas, P. C., Hain, C. R., Semmens, K., Yilmaz, M. T., Gao, F., Otkin, J. A.,  
569 and Tetrault, R.: The Evaporative Stress Index as an indicator of agricultural drought in Brazil: An  
570 assessment based on crop yield impacts, *Remote Sensing of Environment*, 174, 82-99,  
571 <https://doi.org/10.1016/j.rse.2015.11.034>, 2016.
- 572 Bakke, S. J., Ionita, M., and Tallaksen, L. M.: The 2018 northern European hydrological drought and its  
573 drivers in a historical perspective, *Hydrology and Earth System Sciences Discussions*, 1-44,  
574 <https://doi.org/10.5194/hess-24-5621-2020>, 2020., 2020.
- 575 Barker, L. J., Hannaford, J., Parry, S., Smith, K. A., Tanguy, M., and Prudhomme, C.: Historic hydrological  
576 droughts 1891–2015: systematic characterisation for a diverse set of catchments across the UK,  
577 *Hydrology and Earth System Sciences*, 23, 4583-4602, <https://doi.org/10.5194/hess-23-4583-2019>, 2019,  
578 2019.
- 579 Buitink, J., Swank, A. M., van der Ploeg, M., Smith, N. E., Benninga, H.-J. F., van der Bolt, F., Carranza, C.  
580 D., Koren, G., van der Velde, R., and Teuling, A. J.: Anatomy of the 2018 agricultural drought in The  
581 Netherlands using in situ soil moisture and satellite vegetation indices, *Hydrology and Earth System  
582 Sciences Discussions*, 1-17, <https://doi.org/10.5194/hess-24-6021-2020>, 2020, 2020.
- 583 Buras, A., Rammig, A., and Zang, C. S.: Quantifying impacts of the 2018 drought on European ecosystems  
584 in comparison to 2003, *Biogeosciences*, 17, 1655-1672, <https://doi.org/10.5194/bg-17-1655-2020>, 2020,  
585 2020.
- 586 Carsel, R. F., and Parrish, R. S.: Developing joint probability distributions of soil water retention  
587 characteristics, *Water resources research*, 24, 755-769, <https://doi.org/10.5194/bg-17-1655-2020>, 2020,  
588 1988.
- 589 Cavus, Y., and Aksoy, H.: Spatial drought characterization for Seyhan River basin in the Mediterranean  
590 region of Turkey, *Water*, 11, 1331, <https://doi.org/10.3390/w11071331>, 2019.
- 591 Ciais, P., Reichstein, M., Viovy, N., Granier, A., Ogee, J., Allard, V., Aubinet, M., Buchmann, N., Bernhofer,  
592 C., and Carrara, A.: Europe-wide reduction in primary productivity caused by the heat and drought in  
593 2003, *Nature*, 437, 529-533, <https://doi.org/10.1038/nature03972>, 2005.
- 594 DWD Climate Data Center (CDC): Historical daily station observations (temperature, pressure,  
595 precipitation, sunshine duration, etc.) for Germany, version v21.3, 2021.  
596 ([https://www.dwd.de/DE/Home/home\\_node.html](https://www.dwd.de/DE/Home/home_node.html))
- 597 Fathian, F., Dehghan, Z., and Vaheddoost, B.: Severity, Duration, and Magnitude Regionalization of  
598 Standardized Precipitation Index Over Iran During 1993-2016, [https://doi.org/10.21203/rs.3.rs-  
599 791764/v1](https://doi.org/10.21203/rs.3.rs-791764/v1), 2021.
- 600 Graf, A., Klosterhalfen, A., Arriga, N., Bernhofer, C., Bogen, H., Bornet, F., Brüggemann, N., Brümmer, C.,  
601 Buchmann, N., and Chi, J.: Altered energy partitioning across terrestrial ecosystems in the European  
602 drought year 2018, *Philosophical Transactions of the Royal Society B*, 375, 20190524,  
603 <https://doi.org/10.1098/rstb.2019.0524>, 2020.





- 604 Gudmundsson, L., and Seneviratne, S. I.: European drought trends, Proceedings of the International  
605 Association of Hydrological Sciences, 369, 75-79, 2015.
- 606 Guha-Sapir, D.: Annual Disaster Statistical Review 2014: The Numbers and Trends. Brussels: CRED; 2015,  
607 in, 2015.
- 608 Guha-Sapir, D., Below, R., and Hoyois, P.: EM-dat: the OFDA/CRED international disaster database,  
609 Universite Catholique de Louvain ([www.emdat.be](http://www.emdat.be)), 2015.
- 610 Hamed, K. H., and Rao, A. R.: A modified Mann-Kendall trend test for autocorrelated data, Journal of  
611 hydrology, 204, 182-196, [https://doi.org/10.1016/S0022-1694\(97\)00125-X](https://doi.org/10.1016/S0022-1694(97)00125-X), 1998.
- 612 Hao, Z., and AghaKouchak, A.: A nonparametric multivariate multi-index drought monitoring framework,  
613 Journal of Hydrometeorology, 15, 89-101, <https://doi.org/10.1175/JHM-D-12-0160.1>, 2014.
- 614 Huang, Y., Hendricks Franssen, H. J., Herbst, M., Hirschi, M., Michel, D., Seneviratne, S. I., Teuling, A. J.,  
615 Vogt, R., Detlef, S., and Pütz, T.: Evaluation of different methods for gap filling of long - term actual  
616 evapotranspiration time series measured by lysimeters, Vadose Zone Journal, 19, e20020,  
617 <https://doi.org/10.1002/vzj2.20020>, 2020.
- 618 KNMI: Daily weather data in the Netherlands, 2021. (<https://www.knmi.nl/nederland-nu/klimatologie/daggegevens>)
- 620 Kleine, L., Tetzlaff, D., Smith, A., Wang, H., and Soulsby, C.: Using water stable isotopes to understand  
621 evaporation, moisture stress, and re-wetting in catchment forest and grassland soils of the summer  
622 drought of 2018, Hydrology and Earth System Sciences, 24, 3737-3752, 1027-5606,  
623 <https://doi.org/10.5194/hess-24-3737-2020>, 2020, 2020.
- 624 Laaha, G., Gauster, T., Tallaksen, L., Vidal, J.-P., Stahl, K., Prudhomme, C., Heudorfer, B., Vlnas, R., Ionita,  
625 M., and Van Lanen, H. A.: The European 2015 drought from a hydrological perspective, Hydrology and  
626 Earth System Sciences, <https://doi.org/10.5194/hess-21-3001-2017>, 2017, 2017.
- 627 McKee, T. B., Doesken, N. J., and Kleist, J.: The relationship of drought frequency and duration to time  
628 scales, Proceedings of the 8th Conference on Applied Climatology, 1993, 179-183,
- 629 Mishra, A. K., and Singh, V. P.: A review of drought concepts, Journal of hydrology, 391, 202-216,  
630 <https://doi.org/10.1016/j.jhydrol.2010.07.012>, 2010.
- 631 Mishra, A. K., and Singh, V. P.: Drought modeling—A review, Journal of Hydrology, 403, 157-175,  
632 <https://doi.org/10.1016/j.jhydrol.2011.03.049>, 2011.
- 633 Mühr, B., Kubisch, S., Marx, A., Stötzer, J., Wisotzky, C., Latt, C., Siegmann, F., Glattfelder, M., Mohr, S.,  
634 and Kunz, M.: Dürre & Hitzewelle Sommer 2018 (Deutschland), Report, 2018.
- 635 Mukherjee, S., Mishra, A., and Trenberth, K. E.: Climate change and drought: a perspective on drought  
636 indices, Current Climate Change Reports, 4, 145-163 %@ 2198-6061, <https://doi.org/10.1007/s40641-018-0098-x>, 2018.
- 637



- 638 Orłowsky, B., and Seneviratne, S. I.: Elusive drought: uncertainty in observed trends and short-andlong-  
639 term CMIP5 projections, *Hydrology and Earth System Sciences*, 17, 1765-1781,  
640 <https://doi.org/10.5194/hess-17-1765-2013>, 2013, 2013.
- 641 Palmer, W. C.: Meteorological drought, US Department of Commerce, Weather Bureau, 1965.
- 642 Pokhrel, Y., Felfelani, F., Satoh, Y., Boulange, J., Burek, P., Gädeke, A., Gerten, D., Gosling, S. N., Grillakis,  
643 M., and Gudmundsson, L.: Global terrestrial water storage and drought severity under climate change,  
644 *Nature Climate Change*, 11, 226-233, 1758-6798, <https://doi.org/10.6084/m9.figshare.13218710>, 2021.
- 645 Samaniego, L., Thober, S., Kumar, R., Wanders, N., Rakovec, O., Pan, M., Zink, M., Sheffield, J., Wood, E.  
646 F., and Marx, A.: Anthropogenic warming exacerbates European soil moisture droughts, *Nature Climate*  
647 *Change*, 8, 421-426 %@ 1758-6798, <https://doi.org/10.1038/s41558-018-0138-5>, 2018.
- 648 Sen, P. K.: Estimates of the regression coefficient based on Kendall's tau, *Journal of the American*  
649 *statistical association*, 63, 1379-1389, 1968.
- 650 Seneviratne, S., Nicholls, N., Easterling, D., Goodess, C., Kanae, S., Kossin, J., Luo, Y., Marengo, J.,  
651 McInnes, K., and Rahimi, M.: Changes in climate extremes and their impacts on the natural physical  
652 environment, <https://doi.org/10.7916/d8-6nbt-s431>, 2012a.
- 653 Seneviratne, S. I., Lehner, I., Gurtz, J., Teuling, A. J., Lang, H., Moser, U., Grebner, D., Menzel, L., Schroff,  
654 K., and Vitvar, T.: Swiss prealpine Rietholzbach research catchment and lysimeter: 32 year time series  
655 and 2003 drought event, *Water Resources Research*, 48, <https://doi.org/10.1029/2011WR011749>,  
656 2012b.
- 657 Sheffield, J., and Wood, E. F.: Characteristics of global and regional drought, 1950–2000: Analysis of soil  
658 moisture data from off - line simulation of the terrestrial hydrologic cycle, *Journal of Geophysical*  
659 *Research: Atmospheres*, 112, <https://doi.org/10.1029/2006JD008288>, 2007.
- 660 Sheffield, J., Wood, E. F., and Roderick, M. L.: Little change in global drought over the past 60 years,  
661 *Nature*, 491, 435-438, <https://doi.org/10.1038/nature11575>, 2012.
- 662 Šimůnek, J., Van Genuchten, M. T., and Sejna, M.: The HYDRUS-1D software package for simulating the  
663 one-dimensional movement of water, heat, and multiple solutes in variably-saturated media, University  
664 of California-Riverside Research Reports, 3, 1-240, 2005.
- 665 Šimůnek, J., Šejna, M., Saito, H., Sakai, M., and Van Genuchten, M. T.: The HYDRUS-1D software package  
666 for simulating the movement of water, heat, and multiple solutes in variably saturated media, version  
667 4.0: HYDRUS Software Series 3, Department of Environmental Sciences, University of California Riverside,  
668 Riverside, California, USA, 315, 2008.
- 669 Spinoni, J., Naumann, G., Vogt, J., and Barbosa, P.: European drought climatologies and trends based on  
670 a multi-indicator approach, *Global and Planetary Change*, 127, 50-57,  
671 <https://doi.org/10.1016/j.gloplacha.2015.01.012>, 2015.
- 672 Teuling, A. J., Van Loon, A. F., Seneviratne, S. I., Lehner, I., Aubinet, M., Heinesch, B., Bernhofer, C.,  
673 Grünwald, T., Prasse, H., and Spank, U.: Evapotranspiration amplifies European summer drought,  
674 *Geophysical Research Letters*, 40, 2071-2075, <https://doi.org/10.1002/grl.50495>, 2013.



- 675 Theil, H.: A rank-invariant method of linear and polynomial regression analysis, 3; confidence regions for  
676 the parameters of polynomial regression equations, *Indagationes Mathematicae*, 1, 467-482, 1950.
- 677 Van Genuchten, M. T.: A closed - form equation for predicting the hydraulic conductivity of unsaturated  
678 soils, *Soil science society of America journal*, 44, 892-898, 1980.
- 679 Wilhite, D. A., and Glantz, M. H.: Understanding: the drought phenomenon: the role of definitions, *Water*  
680 *international*, 10, 111-120, 1985.
- 681 Yue, S., and Wang, C.: The Mann-Kendall test modified by effective sample size to detect trend in serially  
682 correlated hydrological series, *Water resources management*, 18, 201-218,  
683 <https://doi.org/10.1023/B:WARM.0000043140.61082.60>, 2004.
- 684 Zink, M., Samaniego, L., Kumar, R., Thober, S., Mai, J., Schäfer, D., and Marx, A.: The German drought  
685 monitor, *Environmental Research Letters*, 11, 074002, <https://doi.org/10.1088/1748-9326/11/7/074002>,  
686 2016.
- 687